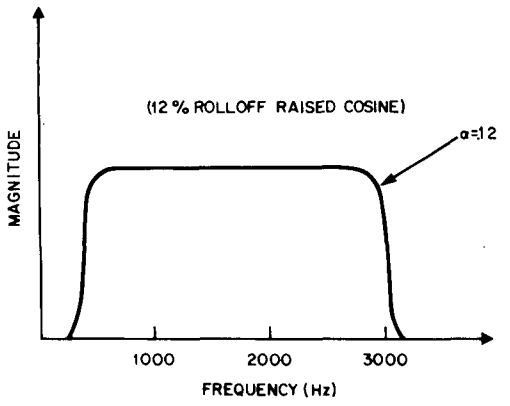

Figure 4. Raised Cosine Transmitter Spectrum.

raised cosine transmitted spectrum shown in Figure 4. No decision errors were experienced in an interval of 2000 symbols compared to 17 errors in the same interval for the structure used in [10]. Furthermore, the effective SNR was 25.4 dB using the phase estimates from the VA. This is superior to the 24.7 dB SNR which was experienced with the receiver using tentative decisions. Because of the large number of operations necessary for the algorithm, the computer simulation of the receiver structure was very time consuming. For this reason no further testing was done but the results are sufficient to give us confidence that over representative telephone channels reliable data transmission at speeds up to 14,400 per second is possible.

IV. CONCLUSIONS

A new algorithm for the simultaneous tracking of phase jitter and detection of data has been developed. Reception of signals from a simulated voiceband channel indicates that good performance can be obtained by this algorithm over typical channels at 14,400 bits/s. For a practical receiver structure, it is likely that some further approximation to this phase-tracking algorithm would be necessary.

ACKNOWLEDGMENT

I would like to thank G. J. Foschini for making helpful suggestions with regard to the algorithm and R. D. Gitlin for some helpful discussions.

REFERENCES

[1] J. Salz, "Optimum Mean-Square Decision Feedback Equalization," *B.S.T.J.*, Vol. 52, No. 8, Oct. 1973, pp. 1341-1373.
[2] D. D. Falconer and G. J. Foschini, "Theory of Minimum Mean Square Error QAM Systems Employing Decision Feedback Equalization," *B.S.T.J.*, Vol. 52, No. 10, December 1973, pp. 1821-1849.
[3] R. Price, "Nonlinearly Feedback-Equalized PAM vs. Capacity for Noisy Linear Channels," *Rec. IEEE Int. Conf. Commun.*, Philadelphia, Pa., June 19-21, 1972.
[4] P. Monsen, "Feedback Equalization for Fading Dispersive Channels," *IEEE Trans. Info. Theory*, IT-17, January 1971.
[5] D. D. Falconer and F. R. Magee, Jr., "Adaptive Channel Memory Truncation for Maximum Likelihood Sequence Estimation," *B.S.T.J.*, Vol. 52, No. 9, November 1973, pp. 1541-1562.
[6] G. J. Foschini, "Performance Bound for Maximum Likelihood Reception of Digital Data," *PGIT*, Vol. IT-21, No. 1, January 1975, pp. 47-50.
[7] S. A. Fredricsson, "Optimum Transmitting Filter in Digital PAM Systems with a Viterbi Detector," *PGIT*, Vol. IT-20, July 1974, pp. 479-489.
[8] S. Qureshi and E. Newhall, "An Adaptive Receiver for Data Transmission Over Time Dispersive Channels." *IEEE Trans. Inform. Theory*, IT-19, July, 1973 pp. 448-457.
[9] F. R. Magee, Jr., "A Comparison of Compromise Viterbi Algorithm and Standard Equalization Techniques Over Band-Limited Channels," *IEEE Trans. Commun.*, Vol. COM-23, March, 1975, pp. 361-367.
[10] D. D. Falconer, F. R. Magee, Jr., "Evaluation of Decision Feedback Equalization and Viterbi Algorithm Detector for Voiceband Data Transmission" Parts I & II, *IEEE Trans. Commun.*, Vol. COM-24, October, 1976, November, 1976.
[11] G. Ungerboeck, "New Application for the Viterbi Algorithm: Carrier-Phase Tracking in Synchronous Data Transmission System," *Rec. IEEE National Telecommunications Conference*, San Diego, Ca., Dec. 2-4, 1974.
[12] H. L. Van Trees, *Detection, Estimation and Modulation Theory*, Part I, New York: Wiley 1968.
[13] "Data Communications Using the Switched Telecommunications Network," *Bell System Technical Reference*, August 1970, pp. 15-16.
[14] J. F. Hayes, "The Viterbi Algorithm Applied to Digital Data Transmission," *The Communications Society Newsletter*, Vol. 13, No. 2, March 1975, pp. 15-20.

Results on Discrete-Time, Decision-Directed Integrated Detection, Estimation, and Identification

JOHN H. PAINTER, SENIOR MEMBER, IEEE,
AND STEPHEN K. JONES, MEMBER, IEEE

Abstract—**New results are presented for symbol-by-symbol detection with decision-directed tracking of colored channel disturbances. Recursive sampled-data algorithms are shown for Maximum *A Posteriori* Probability of detection under colored additive and multiplicative Gaussian noises along with white Gaussian noise. Preliminary evaluation of the algorithms via Monte Carlo simulation shows good performance compared to standard white-noise only algorithms.**

INTRODUCTION

The problem of M-ary detection in channels subject to colored additive and multiplicative disturbances, as well as additive white noise, is reexamined below. New algorithms for symbol-by-symbol detection are obtained from a simplification of the Maximum *A Posteriori* Probability (MAP) strategy for detecting sequences, or blocks, of symbols. A requirement is assumed to process the received waveform on a sample-by-sample (recursive) basis. The algorithms resulting from this requirement yield a new view of the detection process itself. There results an imbedding in the detection algorithms of estimation algorithms for real-time tracking of the colored channel distrubance waveforms. The optimum tracking for detection also requires identification of the statistics (bandwidths,

Paper approved by the Editor for Data Communication Systems of the IEEE Communications Society for publication after presentation at the NAECON, Dayton, OH, May 17–19, 1977. Manuscript received July 21, 1976; revised February 23, 1977. This work was supported in part by the United States Air Force under Contract F-33615-75-C-1011.

The authors are with the Department of Electrical Engineering, Texas A&M University, College Station, TX 77843.

strengths, etc.) of the colored disturbances. Thus, the total process described below is called Integrated Detection, Estimation, and Identification (IDEI).

Early theoretical work on detection in channels perturbed by more than just additive white Gaussian noise [1, 2, 3] led to such developments as the "RAKE" receiver [4] and diversity reception [5]. The idea of adjusting the detector to changing channel conditions led to adaptive detection [6, 7], wherein channel parameters are estimated. An idea dual to adaptive detection, that of estimating the waveform of a signal whose presence is uncertain, was explored in [8, 9]. A related idea, that of differentiating between several possible signals, and simultaneously estimating some signal parameters was explored in [10, 11]. The first recursive sampled-data algorithms for M-ary detection in colored multiplicative noise and white additive noise, using the MAP strategy, were presented in [12]. Simulation results for those algorithms, plus an ad hoc treatment of the required identification problem, were given in [13].

The present paper extends the work in [12] and [13] to include colored additive noise along with colored multiplicative noise, together with white additive noise. Also, the identification problem is formally imbedded into the detection/estimation problem by applying the composite detection strategy. The resulting formal solution to the integrated detection/estimation/identification (IDEI) problem extends the "Marginal ML Estimation" approach of [14] to the detection problem and employs decision-direction estimation [15] to combat the problem of exponentially growing processor memory. The formal solution obtained in this paper is a suboptimal one based on assumed availability of sufficiently good identification of the colored noise statistics. For identification estimates not satisfying the assumption an extended solution based on the "partitioning" approach of [16] is indicated.

In the present paper are presented the first Monte Carlo simulation results for the IDEI algorithms for binary Phase-shift-keying and Frequency-shift-keying, assuming perfect identification of the statistics of the channel disturbances. The error rate performance indicated by the curves in this paper may be viewed as the best performance possible for the IDEI algorithms using standard FSK and PSK signal waveforms. Performance data are presently being gathered and will be reported later for IDEI using practical identification algorithms.

Symbol-by-Symbol Detection

The problem is to detect the occurrence of a transmitted symbol, m, which is the Jth symbol in a sequence. The symbol is an element of the M-ary alphabet, as

$$m \in \{0, 1, \cdots, M-1\}. \tag{1}$$

The decision on m is to be made after a fixed number, K, of received data samples, $\boldsymbol{z}(k)$, has been collected during the present symbol period. It is assumed that information is available from the detection processing over the previous $J-1$ symbol periods.

The data vector, $\boldsymbol{z}(k)$, is assumed to be generated by a state-variable model as shown in Figure 1. Such a model is useful for many different signal forms, as shown in the example below. In Fig. 1, $w(k)$ is a white zero-mean Gaussian noise vector of unit variance. $\boldsymbol{\mu}(k)$ is a deterministic vector. $\Gamma(\,)$, $\Phi(\,)$, and $\Lambda(\,)$ are input, transition, and output matrices of appropriate dimensions. $H_Y(\,)$ and $H_\mu(\,)$ are matrices for introducing modulation into the model. $\boldsymbol{n}(k)$ is an additive

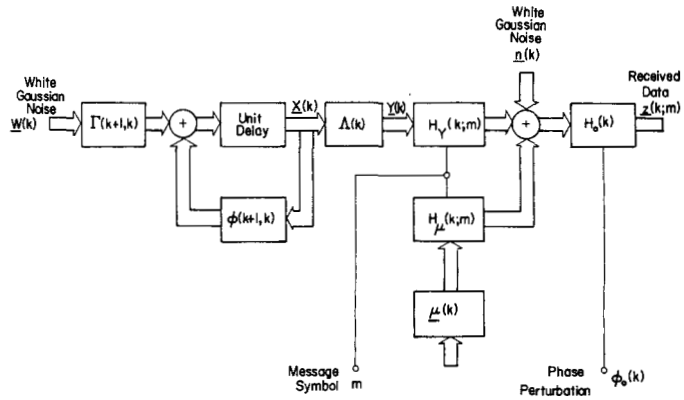

Figure 1. Received Data Generator Model. Characters with underbars are boldface in text.

white, zero-mean, Gaussian noise vector, independent of $\boldsymbol{w}(k)$. The stochastic output vector, $\boldsymbol{Y}(k)$, generated from the state-vector, $\boldsymbol{X}(k)$, accounts for both additive and multiplicative colored noise in the received data, $\boldsymbol{z}(k)$. $H_0(k)$ is a stochastic rotation matrix.

The governing equations for the assumed data generator of Figure 1 are

$$\begin{aligned} \boldsymbol{z}(k) &= H_0(k)[H_Y(k;m)\boldsymbol{Y}(k) + H_\mu(k;m)\boldsymbol{\mu}(k) + \boldsymbol{n}(k)] \\ \boldsymbol{Y}(k) &= \Lambda(k)\boldsymbol{X}(k) \\ \boldsymbol{X}(k+1) &= \Phi(k+1, k)\boldsymbol{X}(k) + \Gamma(k+1, k)\boldsymbol{w}(k). \end{aligned} \tag{2}$$

As an example, the In-phase/Quadrature data channels for a radio signal consisting of a line-of-sight component, diffuse reflection component with multiplicative noise, additive colored noise, and white noise may be modeled, as in (2), by

$$\begin{aligned} \begin{bmatrix} z_I(k) \\ z_Q(k) \end{bmatrix} = {} & \begin{bmatrix} \cos\phi_0(k) & \sin\phi_0(k) \\ -\sin\phi_0(k) & \cos\phi_0(k) \end{bmatrix} \\ & \cdot \left\{ \left[A(k;m) \begin{bmatrix} \cos\phi(k;m) & 0 \\ 0 & \sin\phi(k;m) \end{bmatrix} \right] \right. \\ & \left. \left[\begin{bmatrix} 1 & 0 \\ 0 & 1 \end{bmatrix} \right] \begin{bmatrix} y_r(k) \\ y_j(k) \end{bmatrix} + A(k;m) \right. \\ & \left. \cdot \begin{bmatrix} \cos\phi(k;m) & 0 \\ 0 & \sin\phi(k;m) \end{bmatrix} \begin{bmatrix} 1 \\ 1 \end{bmatrix} \right. \\ & \left. + \begin{bmatrix} n_I(k) \\ n_Q(k) \end{bmatrix} \right\}. \end{aligned} \tag{3}$$

In (3), $\boldsymbol{z}(k)$ is a two-vector with components $z_I(k)$, $z_Q(k)$. $H_0(k)$ is the unitary matrix function of $\phi_0(k)$, a postulated phase perturbation in the I-Q demodulation reference sine wave. $\boldsymbol{Y}(k)$ is a partitioned vector containing $\boldsymbol{y}_r(k)$ and $\boldsymbol{y}_j(k)$, each of which are 2-vectors. $\boldsymbol{y}_r(k)$ represents a multiplicative noise process, produced by a diffuse multipath reflection. $\boldsymbol{y}_j(k)$ represents an additive colored interference. $A(k;m)$ and $\phi(k;m)$ are the envelope and phase functions, respectively, for the transmitted signal, during the Jth symbol interval. $\boldsymbol{\mu}(k)$ is $[1, 1]^T$ in (3), and represents the direct path. $\boldsymbol{n}(k)$ is a two-

vector with components $n_I(k)$ and $n_Q(k)$, which are independent, white, zero-mean, Gaussian, with equal variances.

The two colored processes, $y_r(k)$ and $y_j(k)$, comprising $\boldsymbol{Y}(k)$, are generated according to (2) as independent Gauss-Markov processes. The orders of the Markov processes are set by choosing the dimension of the state vector, $\boldsymbol{X}(k)$, as appropriate to the problem being modeled. The example of equation (3) has been simplified for the sake of clarity. Quasi-specular reflections and/or frequency-selective channels with a delay-spread reflection may be modeled within the framework of (2), but with more structure than in (3).

Given knowledge of the transmitted symbol, m, the matrix sampled-data functions, $H_Y(\ )$ and $H_\mu(\ )$, are known for all sample times, k, in the symbol period. This assumes known symbol timing. The functions $\Gamma(\ )$, $\Phi(\ )$, and $\Lambda(\ )$ are not necessarily known, *A Priori*, since they determine such statistics as strength and band width of the colored channel disturbances in $\boldsymbol{Y}(k)$. The vector $\boldsymbol{\mu}(\ )$ is not known since it represents the strength of any signal components subject only to additive noise. Likewise, the variance matrix, $V_{nn}(k)$, corresponding to the additive white noise, $\boldsymbol{n}(k)$, is not necessarily known. The rotation matrix is assumed known, since $\phi_0(k)$ is assumed to be created in the receiver and, hence, is measurable.

Let a vector, $\boldsymbol{\beta}(k)$, be defined which contains the finite number of unknown elements in $\Gamma(\ )$, $\Phi(\ )$, Λ, $\boldsymbol{\mu}(\ )$, and $V_{nn}(\ )$. $\boldsymbol{\beta}(k)$ is assumed to be either constant or slowly time-varying with respect to the period of a transmitted symbol. The data vector, $\boldsymbol{z}(k)$, is vector-Markov and Gaussian, when conditioned on $\boldsymbol{\beta}(k)$ and m.

The decision on the symbol, m, which is the Jth symbol in a sequence, is made by forming and testing decision statistics, $S(m)$ for each value of $m = 0, 1, \cdots, M-1$. The data processing algorithm which produces the M statistics, $S(m)$, is derived by first considering detection of the symbol sequence as a whole, under the MAP strategy. This entails producing detection statistics

$$S'(m) = p(\mathsf{M}/\mathsf{Z}) \tag{4}$$

where M is the collection of all J symbols in the sequence and Z is the collection of all KJ data samples, $\boldsymbol{z}(\ )$. The function, $p(\ )$, is the conditional probability. Obviously M^J such statistics must be computed and compared to decide on the symbol sequence as a whole.

Because it requires a processor whose size expands exponentially with the length of the message sequence, decision on the sequence as a whole is undesirable. Although short sequences could be tolerated, the approach in this paper is simply to make symbol-by-symbol decisions. In the presence of white noise only, with no channel memory, such a decision strategy is optimum, since data from other symbol periods do not aid detection of the present symbol. However, in the presence of multiplicative or additive colored noise, previous data may be used to improve the present decision. Thus, in the present case, a symbol-by-symbol decision technique is employed which does use information from previous symbol times.

Symbol-by-symbol decision is a recursive procedure with respect to the occurrance of the symbols. Further, however, it is desired to process the data samples recursively within each symbol period. The procedure in deriving the required symbol-by-symbol decision statistics, $S(m)$, for a fully recursive processor is straightforward, but notationally tiring, especially to the reader not used to discrete-time state-variable models. For the interested reader, the derivation is recorded in Reference [17]. The final resulting algorithm is given as

$$S(m) = p(m \mid \hat{\mathsf{M}}) \cdot \prod_K \left[p(\boldsymbol{z}(k) \mid m, \hat{\boldsymbol{\beta}}(k \mid k-1), \hat{\mathsf{M}}, \hat{\mathsf{B}}, \mathsf{Z}) \right] \tag{5}$$

In equation (5), $p(m \mid \hat{\mathsf{M}})$ is a conditional probability of the occurrence of the present symbol, m, given the estimate (by decision), $\hat{\mathsf{M}}$, of all the previous symbols in the sequence. The product, π, is over the K sample times in the present symbol period. The probability density function, $p(\boldsymbol{z}(k) \mid (\ ))$, is a conditional density on the received data vector at sample number k, within the present symbol period. The conditioning variable, m, is one of the M possible values of the symbol. $\hat{\boldsymbol{\beta}}(k \mid k-1)$ is a conditional-mean estimate of the unknown channel structure at sample number k, given all the received data samples from sample number $k-1$ backward in time to the beginning of the symbol sequence. The $\hat{\boldsymbol{\beta}}(\ )$ estimator is decision-directed at the beginning of each symbol period. $\hat{\mathsf{B}}$ is the collection of all decision-directed filtered estimates, $\hat{\boldsymbol{\beta}}(k-1 \mid k-1)$. Z is the collection of all data vectors, backward in time, commencing with $\boldsymbol{z}(k-1)$.

Equation (5) was obtained by application of the composite detection strategy, averaging an intermediate decision statistic over the stochastic $\boldsymbol{\beta}(\ )$ vectors. An assumption was employed that the estimates $\hat{\boldsymbol{\beta}}(k \mid k-1)$ and $\hat{\boldsymbol{\beta}}(k-1 \mid k-1)$ have suitably small variances. As the variances of the identification estimates increase it can be expected that the performance of the detection algorithms will degrade. If sufficiently good identification estimates cannot be obtained, then an algorithm should be used, based on the Partitioning Theorem of [16].

With the data generated as in (2) and under the above assumptions on the composition of $\boldsymbol{\beta}(k)$, the density, $p(\boldsymbol{z}(k) \mid (\ ))$, required in the detection algorithm of (5) is conditionally Gaussian, of the form

$$\begin{aligned} p(\boldsymbol{z}(k) \mid (\ )) &= \frac{1}{2\pi} \left[\det V_{\nu\nu}(k \mid k-1)\right]^{-1/2} \\ &\quad \cdot \exp\left[-\tfrac{1}{2} \boldsymbol{\nu}^T(k) V_{\nu\nu}^{-1}(k \mid k-1) \boldsymbol{\nu}(k)\right] \\ \boldsymbol{\nu}(k) &= \boldsymbol{z}(k) - \hat{\boldsymbol{z}}(k \mid k-1) \\ \hat{\boldsymbol{z}}(k \mid k-1) &= E\{\boldsymbol{z}(k) \mid (\ )\} \\ V_{\nu\nu}(k \mid k-1) &= E\{\boldsymbol{\nu}(k)\boldsymbol{\nu}^T(k) \mid (\ )\}. \end{aligned} \tag{6}$$

When $\boldsymbol{z}(k)$ is conditioned on the m truly present, $\boldsymbol{\nu}(k)$ is the Innovations Process [18]. In computing the M statistics, $S(m)$, as in (5), the true m is used in only one of the $\boldsymbol{\nu}(k)$. Thus, $\boldsymbol{\nu}(k)$ is called here the Pseudo-Innovations. Since $\boldsymbol{z}(k)$ is conditionally Gaussian, both $\boldsymbol{\nu}(k)$ and $V_{\nu\nu}(k \mid k-1)$ may be obtained from Kalman filters. In the Kalman filter, $\boldsymbol{\nu}(k)$ is the dynamic feedback tracking error, formed in the filter. Each filter attempts to track $\boldsymbol{Y}(k)$, the vector of colored channel disturbances.

The physical operation of the optimum detection algorithms is now explained, with reference to Figures 2 and 3.

During the Jth symbol period, M unique detection statistics $S(m)$ are computed in parallel, one for each of the possibly present m. Each separate statistic generator contains its own Linear (Kalman) Filter, Gaussian Function Generator, Conditional-Mean Predictor/Filter, and Product Accumulator.

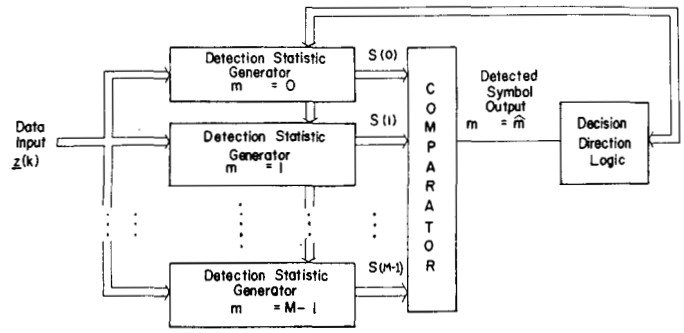

Figure 2. Decision-Directed MAP Detector (IDEI). Characters with underbars are boldface in text.

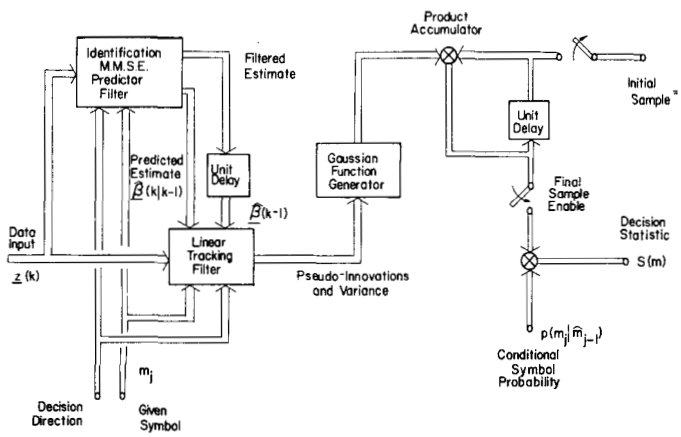

Figure 3. Detection Statistic Generator. Characters with underbars are boldface in text.

At the end of the Jth symbol period, the nonnegative statistics, $S(m)$, are compared in magnitude. If $S(n)$ is largest, then the decision is made $\hat{m} = n$.

At the end of the Jth symbol period, the decision direction feature is employed as follows. When the decision is made, $\hat{m} = n$, it is inferred that the nth detection statistic generator has been processing the data using the true value of m. Thus, it is inferred that the Kalman filter and Conditional-Mean Identifying filter in the nth statistic generator contain good final filtered estimates, $\hat{X}(JK)$, and $\hat{\beta}(JK)$, respectively. These final filtered estimates are then routed to the other $M - 1$ statistic generators to reset their initial predicted estimates for the $(J + 1)$st symbol period.

The present results on discrete-time detection theory are also quite analogous to some previous continuous-time work of Kailath [19], concerning the Likelihood Ratios (LR) for detection of binary random signals in Gaussian noise. The problem analyzed by Kailath was initially that of detection of an "on-off keyed" (OOK) colored stochastic signal in white Gaussian noise. The continuous-time formulation for the LR was

$$\mathrm{LR} = \exp\left[\oint_0^T \hat{y}(t)\, z(t)\, dt - \frac{1}{2}\int_0^T \hat{y}^2(t)\, dt\right] \tag{7}$$

where $z(t)$ was the observed data process on the time interval $[0, T]$ and $\hat{y}(t)$ was the causal conditional-mean estimate of the colored signal, under the conditioning that the signal was present. The barred integral denotes the stochastic Ito integral.

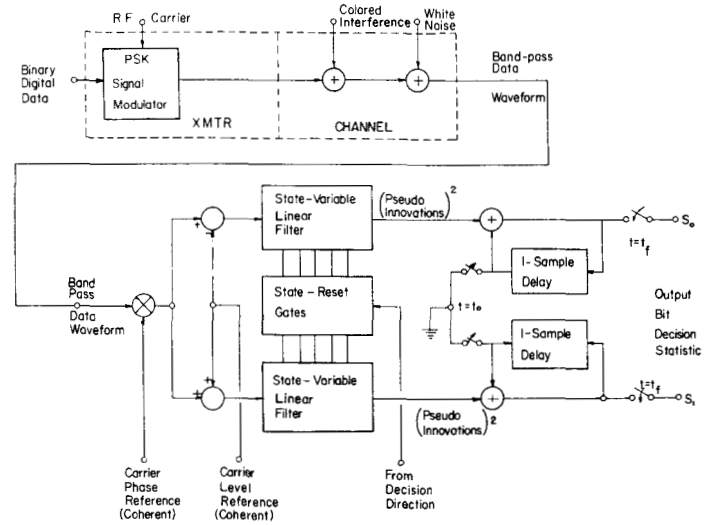

Figure 4. Interference-Tracking PSK Detector.

The limiting discrete-time result as the sampling becomes dense in the $[0, T]$ interval for Kailath's problem, using the approach of the present paper, is

$$\mathrm{LR} = \exp\left[\sum_{k=1}^{\infty} \hat{y}(k \mid k-1) z(k) - \frac{1}{2}\sum_{k=1}^{\infty} \hat{y}^2(k \mid k-1)\right]. \tag{8}$$

The correspondence to Kailath's result is clear. For practical implementations, the summation index will remain finite and no convergence difficulties will exist.

Example

Figures 4 and 5 relate to a highly simplified example, presented here to clarify some of the preceding ideas. Assume binary phase-shift-keying with $\pm 90^\circ$ phase shift in the presence of an additive colored interference process and white noise. No multiplicative channel disturbance is assumed. Also, postulate phase coherent translation of the band-pass data to baseband, using an unperturbed phase reference (a highly idealized case). Under these assumptions, the desired signal is resident in the quadrature channel only, and the data are scalar, continuous-time, taken here as $z(t)$. Instead of Kalman filters, suboptimum stationary Wiener filters may be postulated in the feedback canonical form of Figure 5. If Charge-Coupled-Device[1] implementation is assumed for these filters, then the conversion from continuous time to discrete time is inherent in the filter structure.

For this example, the components of (2) are

$$H_0(k) = 1$$

$$H_Y(k; m) = 1$$

$$\boldsymbol{Y}(k) = y_j(k): \qquad \text{a scalar function}$$

$$H_\mu(k; m = 0) = +A: \qquad 0 < A$$

[1] The recursive structure indicated in Figure 5 is not the usual CCD transversal filter structure common to the CCD art. The state-variable feed-back structure is required so that the states may be reset at the end of each symbol period. The design of such a CCD device is presently being pursued at Texas A&M University.

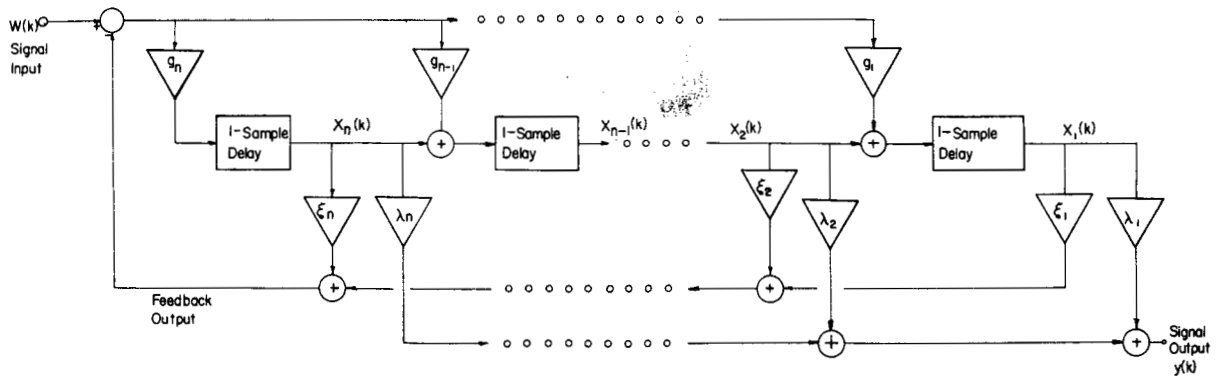

Figure 5. Recursive State-Variable Filter.

$$H_\mu(k; m = 1) = -A$$

$$\mu(k) = 1$$

$$n(k) = n(k): \quad \text{a scalar function.} \tag{9}$$

The required identification for this example includes the carrier reference level, A, and the set of constants in $\{\Gamma(\,), \Phi(\,), \Lambda(\,)\}$. Identifying $\{\Gamma(\,), \Phi(\,), \Lambda(\,)\}$ is essentially identifying the power spectrum of the colored additive interference (not necessarily narrow band) and then synthesizing a suitable minimum-phase recursive filter for tracking $y_j(k)$.

In Figure 5, the upper filter is for $m = 0$. The lower filter is for $m = 1$. In the upper channel, $\hat{A}$ is subtracted from the scalar data when $m = 0$. In the lower channel $(-\hat{A})$ is subtracted from the scalar data to produce $y_j(k) + n(k)$ when $m = 1$. Each filter then attempts to track $y_j(k)$ under the differing assumptions on m. For this case the sum of the squares of the pseudoinnovations forms a sufficient statistic for detection. Thus, the sum of squares is accumulated recursively using the scheme shown in Figure 4. After each symbol decision the final states in the incorrect filter are reset using the final states in the correct filter.

It can be seen clearly from this example that the "correct" filter is driven simply by the colored interference plus white noise, since the desired signal waveform has been subtracted out of the in-coming data. Moreover, the filter is optimized to track the colored waveform with minimum mean-squared error. Thus, theoretically there is no restriction on use of the algorithm due to colored interference bandwidth. This detector will, in fact, operate with colored interference whose power spectrum exactly overlays the spectrum of the desired signal, albeit with greater error rate than for narrow-band interference. All that is required is that the colored interference and desired signal be uncorrelated.

It can also be seen that the statistic produced by the "incorrect" filter is larger due to that filter's error response to the difference of the two possible desired signals.

Thus, closed-form numerical evaluations of the error-rate performance of the IDEI detector must necessarily be made for particular interference cases. The present paper shows some Monte Carlo simulation evaluations of error rate performance, leaving closed-form results for subsequent reporting.

SIMULATION RESULTS

Reported herein are the first simulation results for the IDEI binary detection for Frequency-Shift-Keying (FSK) and for Phase-Shift-Keying (PSK). The simulation is structured as per Figure 6. In operation, the Message Generator produces a sequence of independent binary digits in the zero/one alphabet. The Modulation Generator produces either a PSK or FSK waveform with continuous phase. The modulation indices are selectable for either PSK or FSK.

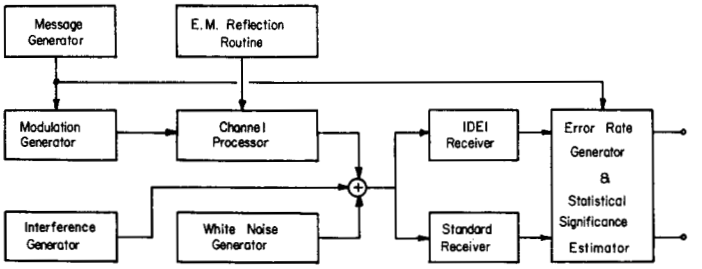

Figure 6. Computer Simulation Structure.

The signal modulation is routed through a Channel Processor which may provide a delayed diffuse multipath with Doppler-spreading colored multiplicative noise and/or delay-spreading filtering, in addition to an unperturbed direct path. The parameters of the Channel Processor are set according to the results of a computerized solution of the rough surface electromagnetic bistatic scattering problem.

An Interference Generator produces a zero-mean Gaussian colored noise process with selectable bandwidth and variance. A White Noise Generator produces a zero-mean Gaussian white noise process with selectable variance. All of the stochastic process generators are driven by independent pseudorandom number sequences.

The outputs of the Channel Processor, Interference Generator, and White Noise Generator are summed to produce the simulated data process, which is routed in parallel to the IDEI Receiver and a Standard Receiver. The IDEI Receiver embodies the algorithms of (5) and (6) as illustrated in Figures 2 and 3. The Standard Receiver employs nonadaptive, discrete time, recursive algorithms, as discussed below. The detected symbols at the output of the Optimum and Standard Receivers are compared to the transmitted symbols to derive the error rate curves shown below. A measure of the statistical significance of the error rates is also derived.

The simulation is run entirely in In-phase/Quadrature form. Thus, the various signal and noise sampled-data waveforms are generated and processed in 2-vector form, corresponding to the model of (2). The constant envelope of the modulated signal is normalized to unity. Thus, the signal to noise ratios in the receivers are adjusted by setting the levels of the various interferences.

For the presently reported cases, the symbol rate was chosen to be 2500 per second, which is the same rate as for the previously reported simulation for a quaternary hybrid modulation in multipath [13]. The PSK phase deviation was chosen at 0.785 radians, for a reason to be discussed below. The equivalent phase deviation for FSK was also taken at 0.785 radians, so as to be comparable with the PSK case. Thus, the frequency shifts, with respect to the carrier frequency, were plus and minus 1962.5 Hz, for $m = 0$ and 1, respectively.

The present results were obtained for two particular channel conditions. Either colored multiplicative noise with white additive noise were present or colored plus white additive noises were present but simultaneous colored additive and multiplicative noises were not used. For the multipath case, zero differential group delay was assumed between the direct and unreflected paths. This is equivalent to an assumption of non-frequency-selective fading. The I/Q low-pass components of the multiplicative noise were obtained by passing independent scalar white noise processes through two separate uncoupled low-pass filters, each having the same transfer function. This is equivalent to an assumption that the Doppler spectrum of the unmodulated carrier displays even symmetry about the carrier frequency. The discrete-time filter algorithms were obtained by driving a continuous-time filter with a sampler and Zero-Order-Hold. The continuous-time filter has three adjustable real pole frequencies and one adjustable real zero frequency. For the present results, the pole frequencies were selected as 250 Hz, 625 Hz, and 2500 Hz. The zero frequency was selected as 10,000 Hz, giving the filter an equivalent noise bandwidth (one-sided) of 275.7 Hz. For the present multipath case, no delay-spreading filtering was assumed.

For the colored additive noise case, the same filter structure was used as for multipath, driven by two independent scalar white noise processes. Thus the colored additive spectrum was assumed to be even-symmetric about the carrier frequency with an equivalent width at radio frequencies of 551.4 Hz. The additive white noise consisted of two scalar white noise processes of equal variance which were independent of each other and all the other white noise driving functions.

The standard receiver algorithms produce the required detection statistics recursively as follows, during the Jth symbol period.

PSK:

$$S(k) = z^T(k) \cdot \begin{bmatrix} 0 \\ 1 \end{bmatrix} + S(k-1): \qquad k = (J-1)K+1, \cdots, JK$$
$$S((J-1)K) = 0. \tag{10}$$

The decision rule is

$$0 \leqslant S(JK) \rightarrow m = 0$$
$$S(JK) < 0 \rightarrow m = 1. \tag{11}$$

FSK:

$$a(k; m=0) = z^T(k) \cdot \begin{bmatrix} \cos(\Delta\omega \cdot t(k)) \\ \sin(\Delta\omega \cdot t(k)) \end{bmatrix} + a(k-1; m=0)$$

$$b(k; m=0) = z^T(k) \cdot \begin{bmatrix} \sin(\Delta\omega \cdot t(k)) \\ -\cos(\Delta\omega \cdot t(k)) \end{bmatrix} + b(k-1; m=0)$$

$$a(k; m=1) = z^T(k) \cdot \begin{bmatrix} \cos(\Delta\omega \cdot t(k)) \\ -\sin(\Delta\omega \cdot t(k)) \end{bmatrix} + a(k-1; m=1)$$

$$b(k; m=1) = z^T(k) \cdot \begin{bmatrix} -\sin(\Delta\omega \cdot t(k)) \\ -\cos(\Delta\omega \cdot t(k)) \end{bmatrix} + b(k-1; m=1)$$

$$a((J-1)K; m=i) = b((J-1)K; m=i) = 0: \qquad i = 0, 1$$

$$t(k) = \left[\frac{k-\frac{1}{2}}{K} - \text{Int}\left(\frac{k-\frac{1}{2}}{K}\right)\right] \cdot \frac{1}{2500} \qquad k = (J-1)K+1, \cdots, JK$$

$$\Delta\omega = 2\pi \cdot \frac{0.785}{2500}$$

$$S_i(k) = a^2(k; m=i) + b^2(k; m=i). \tag{12}$$

The decision rule is

$$S_1(K) \leqslant S_0(K) \rightarrow m = 0$$
$$S_0(K) \leqslant S_1(K) \rightarrow m = 1. \tag{13}$$

In order to calibrate the simulation, runs were first made using PSK modulation and white noise only. Results of four runs were plotted in Figure 7 upon the theoretical error rate curve, given by

$$P_b(e) = \frac{1}{2}\left[1 - \text{erf}\left(\sqrt{\frac{E(1-p)}{2N_0}}\right)\right]$$

$$E/N_0 = \frac{\frac{1}{2}\sin^2(\Delta\phi)}{\sigma_n^2/K}; \qquad \rho = -1; \text{PSK}$$

$$E/N_0 = \frac{1 - \frac{1}{K}\sum_{k=1}^{K}\cos^2\left(\frac{2\pi}{K}\left(k-\frac{1}{2}\right)\Delta\phi\right)}{\sigma_n^2/K};$$

$$\rho = 0: \text{FSK}. \tag{14}$$

In (14) K is the number of samples per symbol (taken here as (10)), $\Delta\phi$ is equivalent phase deviation in radians, and σ_n^2 is the variance of each scalar component of the I-Q white noise 2-vector. Not only did the simulated error rates fall on the theoretical PSK curve, but the standard PSK detector and the IDEI detector made precisely the same errors, symbol for symbol.

In attempting to obtain simulation results for PSK in multiplicative noise, it was observed that the error rate was 0.5 for all values of E/N_0. In retrospect, this behavior may be predicted analytically. To remedy this situation, the signal phase deviation was reduced from $\pi/2$ radians in order to produce an unmodulated carrier component in the transmitted signal. Such a component serves as a channel probe and enables the optimum detector to track the multiplicative noise. Figure 8 shows the minimization of the error rate as a function of phase deviation.

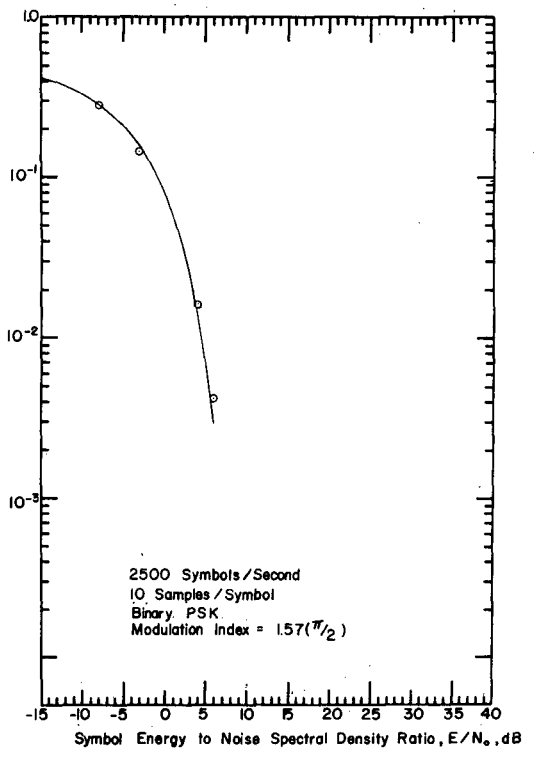

Figure 7. Simulated Error Rate Check Case–White Noise Only.

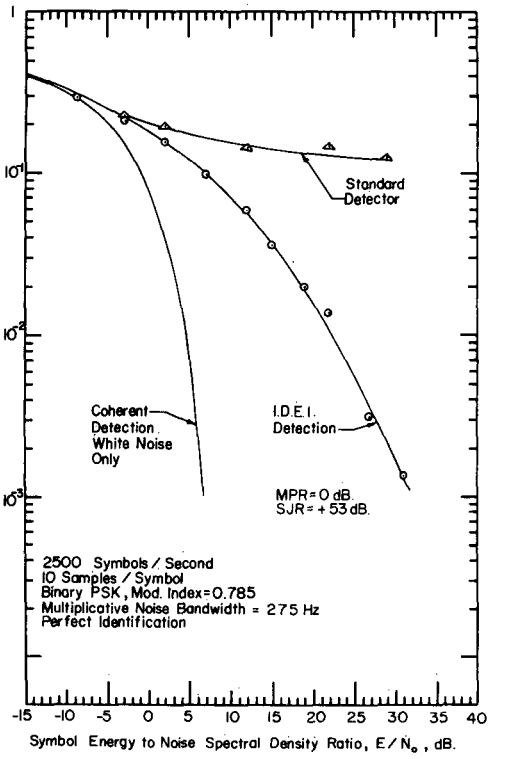

Figure 9. Simulated Error Rate–PSK and Multiplicative Noise.

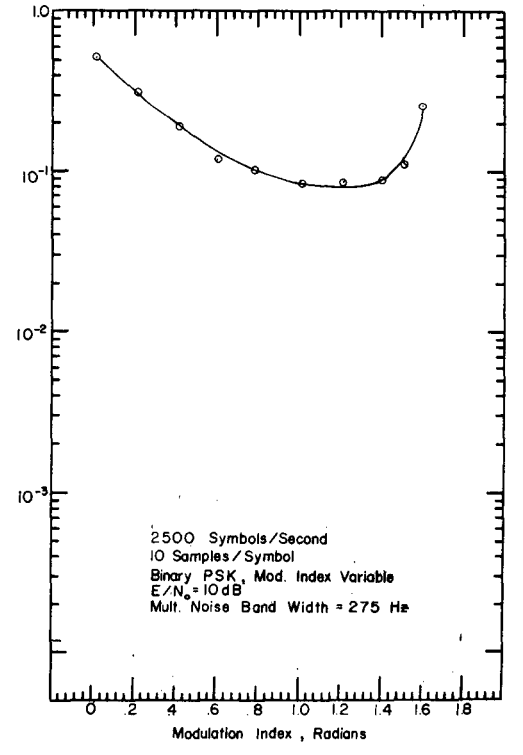

Figure 8. Minimization of Error Rate Versus Modulation Index.

Simulation runs were made for both PSK and FSK with either multiplicative noise or additive colored noise interference. For these runs, the IDEI detection algorithms of (5) and (6) were used without using the Identification Predictor/Filter shown in Figure 3. Rather, the Kalman filter was implemented with the exact components, $\Gamma(\,)$, $\Phi(\,)$, $\Lambda(\,)$, $\mu(\,)$, $H_Y(\,)$, $H_\mu(\,)$, and σ_n^2 used to generate the data as per (2) and Figure 1. Thus, the IDEI detector was furnished with "perfect identification" of the statistics of the channel. For these runs, $H_0(\,)$ was set to the 2×2 identity matrix. Thus, the data were generated without any phase perturbations in the I-Q demodulator. Perfect symbol synchronization and no quantization of the data waveforms were assumed. These runs served to determine the greatest lower bound for the error rate of the IDEI detector, without possible degradation due to imperfect identification estimators.

As the simulation progresses, a raw error rate is computed recursively from the transmitted and detected message symbols. From the raw error rate, recursive estimates of the mean and variance of the error probabilities are computed using vanishing memory estimators. Two different convergence tests are used jointly to terminate the simulation run. The first test is that the ratio of sample-mean value of error rate to sample standard deviation must be greater than 10. The second test is that the ratio of the difference of the last two sample-mean error rates to the last sample-mean error rate must be less than 10^{-4}. It is generally the last Cauchy convergence criterion which terminates the simulation run. This simulation routine has been devised for running on minicomputers with limited memory. The trade-off is that long run times are required.

Results for PSK with multiplicative noise are shown in Figure 9. The multiplicative noise level is set as though the diffuse reflected path were equal in strength to the direct path. Additive colored noise is set 53 dB below the direct path signal level. The standard detector error rate saturates at an irreducible level approximating 10^{-1}. The IDEI detector error rate decreases exponentially with increasing E/N_0.

Figure 10 shows results for PSK with colored additive noise. The multipath is set 47 dB below the direct path signal. The colored noise is set equal in power to the direct path signal. The standard detector operates at an irreducible error

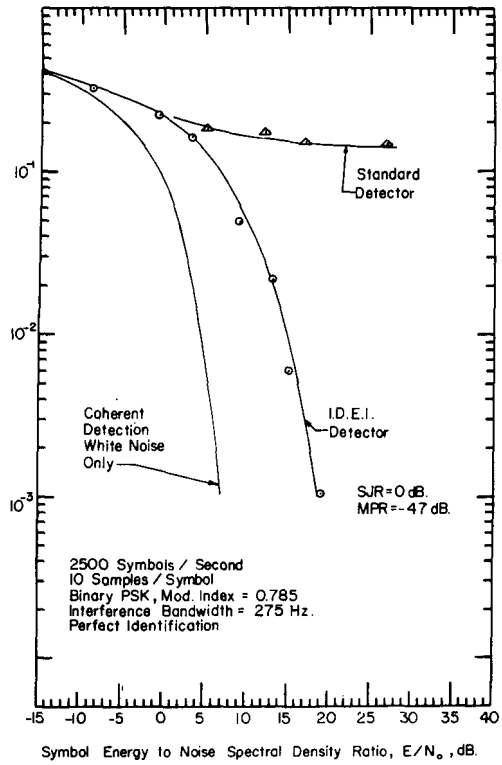

Figure 10. Simulated Error Rate—PSK and Colored Interference.

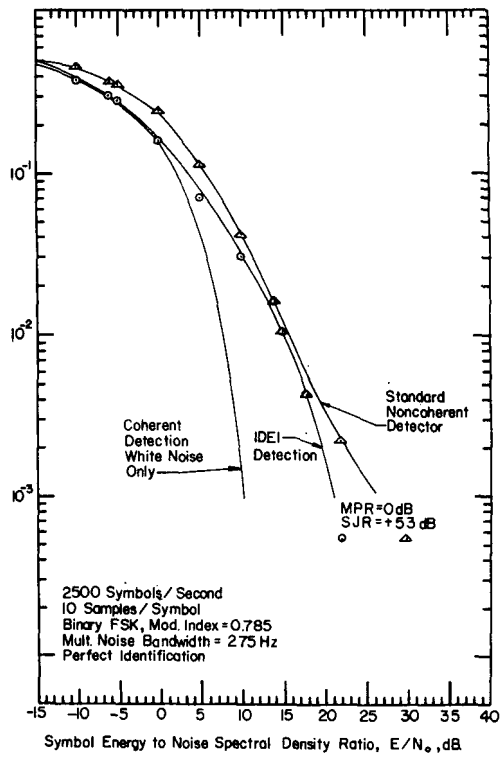

Figure 11. Simulated Error Rate—FSK and Multiplicative Noise.

rate level, similar to the multipath results. The IDEI detector error rate decreases exponentially with increasing E/N_0; however the penalty in E/N_0 is not as large as in the multipath case. The slope of the optimum error rate curve appears to approach that of the white noise only case.

Figure 11 shows the results for FSK with multipath of the same strength as for the PSK case. It is apparent that FSK is a more robust modulation than PSK in multiplicative noise, since both the standard detector and optimum detector perform markedly better than in the PSK case. For error rates greater than 10^{-3}, the standard detector performs almost as well as the optimum detector. Divergence in performance between the two detectors can be seen beginning for error rates less than 10^{-3}.

Figure 12 shows the results for FSK with additive colored noise of the same strength as for the PSK case. Here again the standard detector performs considerably better than in the PSK case. However, the optimum detector comparison is much more impressive. For PSK at 10^{-3} error rate, the additive colored noise was equivalent to a 12 dB increase in the white noise level. For FSK at 10^{-3} error rate, the same colored noise is equivalent to only a 1 dB increase in white noise level. Part of the explanation for the better performance of FSK over PSK in this simulation is that the 550 Hz wide additive interference sits between the two FSK tones. If the colored noise were wider the FSK performance would decrease. For PSK, the interference sits in the maximum portion of the PSK signal spectrum. This superiority should not be expected for wider bandwidth colored interference.

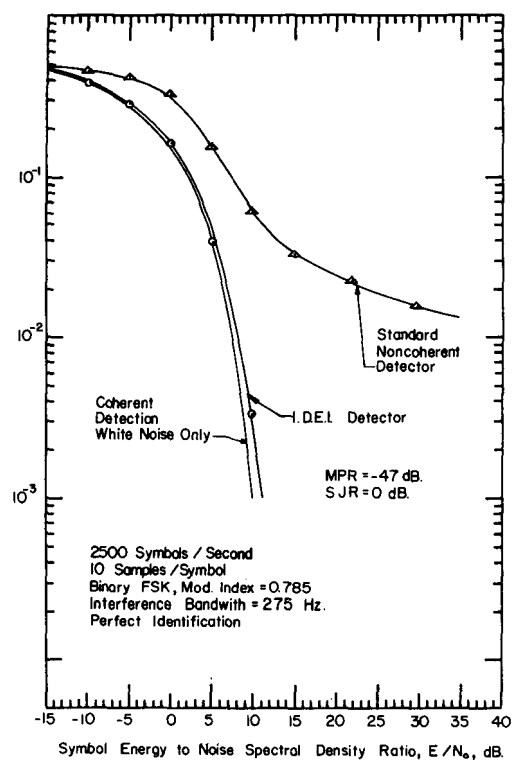

Figure 12. Simulated Error Rate—FSK and Colored Interference.

CONCLUSION

This paper has presented new recursive sampled-data algorithms for M-ary MAP detection in channels subject to both additive and multiplicative colored noise, as well as additive white noise. The recursive formulation formally resulted in the imbedding of M.M.S.E. tracking and identification of the colored disturbances in the detection algorithms. Although hard symbol decisions were used in the present work, the decisions are not independent from symbol to symbol, since decision-directed disturbance tracking is employed.

The recursive algorithms provide a different view of the detection problem, especially for additive colored and white noise. For instance, it seems that the error rate is not controlled by the power of the additive colored disturbance directly, but only by the mean-squared-error of the filter which tracks the disturbance. Also, the colored disturbances, multiplicative or additive, are not restricted to be narrow-band with respect to the desired signal.

The IDEI algorithms yield gain against colored disturbances, for standard modulations without spectrum spreading. Where standard detector error rates saturate, the IDEI error rate, at least for perfect identification, decreases rapidly with decreasing white noise level.

Whether these new theoretical results become of practical interest hinges on the answers to two key questions. The key theoretical question is, "What identification accuracy is required to produce acceptable error rates with the new algorithms?" The key practical question is, "Can low-cost linear tracking filters with sufficient processing speed be implemented in hardware?" The answer to the hardware question depends on the nature of the channel itself. For colored channel disturbances with bandwidths less than, say 1 kHz, digital filter implementation seems indicated. For wide bandwidth channel disturbances, hybrid processing hardware, perhaps employing CCD devices, may be the answer.

REFERENCES

[1] G. L. Turin; "Communication through noisy random multipath channels," in *IRE Conv. Rec.*, Pt. 4, March 1956, pp. 154-166.

[2] Price, R.; "Optimum detection of random signals in noise, with application to scatter-multipath communication, I," *IRE Trans. Inform. Theory*, Vol. IT-2, pp. 125-135, December 1956.

[3] Kailath, T.; "Correlation detection of signals perturbed by a random channel," *IRE Trans. Inform. Theory*, Vol. IT-6, pp. 361-366, June 1960.

[4] Price, R. and Green, P. E.; "A communication technique for multipath channels," *Proc. IRE*, Vol. 46, pp. 555-570, March 1958.

[5] Pierce, J. N.; "Theoretical diversity improvement in frequency-shift keying," *Proc. IRE*, Vol. 46, pp. 903-910, May 1958.

[6] Hancock, J. C. and Lindsey, W. C.; "Optimum performance of self-adaptive systems operating through a Rayleigh-fading medium," *IEEE Trans. on Commun. Syst.*, Vol. CS-11, pp. 443-453, Dec. 1963.

[7] Esposito, R., Middleton, D., and Mullen, J. A.; "Advantages of amplitude and phase adaptivity in the detection of signals subject to slow Rayleigh fading," *IEEE Trans. Inform. Theory*, Vol. IT-11, pp. 473-482, October 1965.

[8] Nahi, N. E.; "Optimal Recursive Estimation with Uncertain Observation," *IEEE Trans. Inform. Theory*, Vol. IT-15, pp. 457-462, July 1969.

[9] Lainiotis, D. G.; "Joint Detection, Estimation, and System Identification," *Information and Control*, Vol. 19, pp. 75-92, 1971.

[10] Middleton, D. and Esposito, R.; "Simultaneous optimum detection and estimation of signals in noise," *IEEE Trans. Inform. Theory*, Vol. IT-14, pp. 434-444, May 1968.

[11] Fredridsen, A., Middleton, D., and Vandelinde, D.; "Simultaneous Signal Detection and Estimation under Multiple Hypotheses," *IEEE Trans. Inform. Theory*, Vol. IT-18, pp. 607-614, Sept. 1972.

[12] Painter, J. H., and Gupta, S. C.; "Recursive ideal observer detection of known M-ary signals in multiplicative and additive Gaussian noise," *IEEE Trans. on Commun.*, Vol. COM-21, pp. 948-953, August 1973.

[13] Painter, J. H., and Wilson, L. R.; "Simulation Results for the decision-directed MAP receiver for M-ary signals in multiplicative and additive Gaussian noise," *IEEE Trans. on Commun.*, Vol. COM-22, pp. 649-660, May 1974.

[14] Mehra, R. K.; "Approaches to Adaptive filtering," *IEEE Trans. Auto. Control*, Vol. AC-17, pp. 693-698, October 1972.

[15] Proakis, J. G., Drouilhet, P. R., and Price, R.; "Performance of Coherent detection systems using decision-directed channel measurement," *IEEE Trans. Commun. Syst.*, Vol COM-12, pp. 54-63, March 1964.

[16] Lainiotis, D. G.; "Partitioning: A unifying framework for adaptive systems, I: Estimation," *Proc. IEEE*, Vol. 64, pp. 1126-1143, August 1976.

[17] Painter J. H.; "Low cost anti-jam digital data-links techniques investigations," *Final Report for Phase I, Contract F33615-75C-1011*, Air Force Avionics Laboratory, Wright-Patterson AFB, Ohio, January 1977.

[18] Kailath, T.; "The innovations approach to detection and estimation theory," *Proc. IEEE*, Vol. 58, pp. 680-695, May 1970.

[19] Kailath, T.; "A general likelihood ratio formula for random signals in Gaussian noise," *IEEE Trans. Inform. Theory*, Vol. IT-15, pp. 350-361, May 1969.

Loop-Induced Magnetic Fields with Negligible Side-Lobes

F. W. UMBACH

Abstract—**In schools for the hard-of-hearing where adjacent classrooms are equipped with non-carrier induction loop systems, it is necessary to realize a geometric discrimination between the classroom-fields. One approach to reaching the required 24 dB per meter roll-off at the boundaries is the orthogonal field principle reported first in 1965 by de Boer, Bosman and Joosten (ref. 2, 3, 4). In this paper a method is described and results are given for an heuristic development of this principle in the case of classrooms about 8 m in length with permissible roll-off ranges of 2 m. It is shown that it is also possible to discriminate in a vertical direction if a secondary field at the ceiling is used. The heuristic approach achieves very good results in this case and overcomes the mathematical difficulties arising when the field is calculated analytically.**

I. THE ORTHOGONALITY PRINCIPLE

A single wire loop, as pictured in Fig. 1, gives rise to a vertical field strength as shown in Fig. 2.

Also shown in Fig. 2 is the cross-talk that arises in the adjacent classroom from such a loop. A loop with 6 m diameter has a maximum field strength for 1 m listening-height at about 2 m out of the center of the field. The field strength decreases to zero at 3.2 m out of the center and reaches a second maximum of 4 m distance. This second maximum is 60% of the field strength at the loop's center. At 8 m distance (in the center of the adjacent classroom) the residual field strength is 15%. It is clear from these figures that such a situation is unallowable.

The vertical field strength H_y caused by a current I through a wire on the floor is, at a horizontal distance of x m and at a height of h_L m,

$$H_y = -\frac{I}{2\pi} \frac{x}{x^2 + h_L{}^2} .$$

Paper approved by the Editor for Radio Communication of the IEEE Communications Society for publication without oral presentation. Manuscript received December 14, 1975; revised December 2, 1976.

The author is with the Department of Electrical Engineering, Twente University of Technology, Enschede, The Netherlands.